Journal of Nanobiotechnology

RESEARCH

Open Access

Pectin-Zein-IPA nanoparticles promote functional recovery and alleviate neuroinflammation after spinal cord injury

Xianghang Chen[1,2,3], Beini Wang[2], Abdullah Al Mamun[2], Kaiyi Du[2], Shengfu Wang[2], Qianqian Hu[2], Xinyuan Chen[2], Yang Lu[2], Anyu Du[2], Yueqi Wu[2], Jiaqin Shao[2], Shuangshuang Wang[1], Chang Jiang[1], Kailiang Zhou[4*], Siwang Hu[1*] and Jian Xiao[2,3,4*]

Abstract

Introduction Spinal cord injury (SCI) impairs the balance of gut microbiomes, which further aggravates inflammation in the injured areas and inhibits axonal regeneration. The intestinal microbiome plays an important role in SCI and regulating intestinal microbiome promotes SCI repair. However, current studies have shown that indole-3 propionate (IPA), a metabolite of gut bacteria, can promote axonal regeneration. However, the short half-life of IPA limits its effectiveness. Gut microbiota plays a role in the progression of SCI, but the studies about diet regulates intestinal flora metabolites to improve SCI are still limited and lack guiding significance.

Results The results showed that Pectin-Zein-IPA NPs treatment improves motor function recovery, inhibits the activation of oxidative stress, enhances axonal regeneration and activates AKT/Nrf-2 signaling pathway following SCI. Further analysis showed that Pec-Zein-IPA NPs treatment reduced the intestinal flora metabolite accumulation of L-methionine, and alleviated neuroinflammation by improving autophagy and inhibiting pyroptosis. Pec-Zein-IPA may reduced neuroinflammation after SCI by decreasing the abundance of *Clostridia_UCG-014*, *Clostridia_vadinBB60_group*, *Shewanella* (positively correlated with L-Methionine) and increasing the abundance of *Parasutterella* (negatively correlated with L-Methionine).

Conclusions Our findings provide a strategy for oral drug research in SCI. The results suggest that Pectin-Zein-IPA NPs have potential advantages for treatment and management of SCI. Reducing L-methionine intake may help reduce neuroinflammation after SCI.

*Correspondence:
Kailiang Zhou
zhoukailiang@wmu.edu.cn
Siwang Hu
siwang_h@wmu.edu.cn
Jian Xiao
xfxj2000@126.com

Full list of author information is available at the end of the article

Graphical Abstract

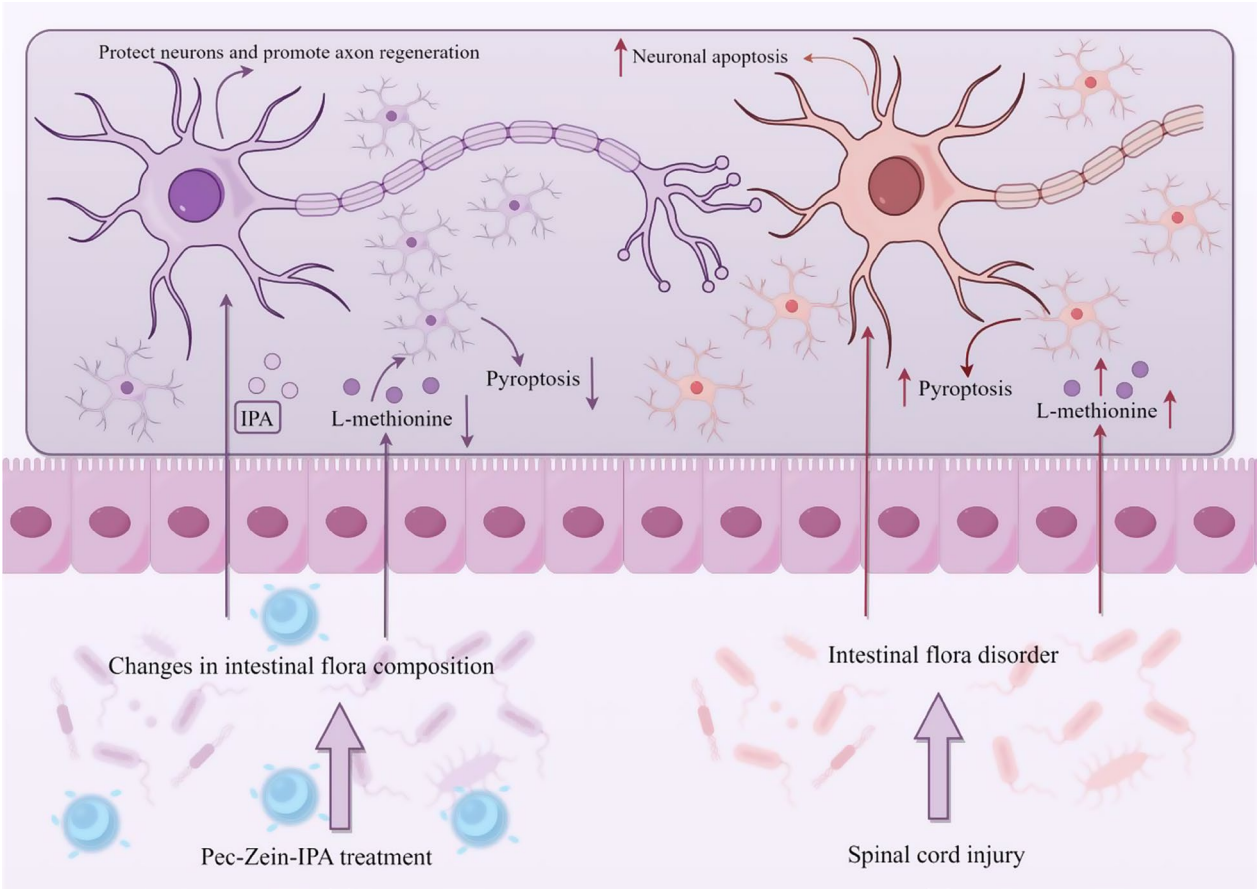

Keywords Spinal cord injury, Indole-3 propionate, Pectin, Zein, Microbiome metabolite

Introduction

Spinal cord injury (SCI) induces loss of sensory and motor functions and burdens patients and families worldwide [1]. SCI causes an imbalance in the intestinal microbes, leading to leaky intestines, which trigger pathogenic bacteria and endotoxins including LPS, entering blood circulation and aggravating neurological conditions [2–5].

Accumulating studies have demonstrated that gut microbes play a crucial role in the functions of the central nervous system (CNS) including neurodevelopment, the synthesis of neurotransmitters, the formation of blood-brain barrier and the maturation of glial cells [6–8]. SCI requires long-term intervention and repair. Therefore, diet regulats gut microbiota to improve injured site microenvironment is an attractive treatment strategy. In ancient China, the earliest food therapy can be traced back to 621 ~ 713 years of the Tang Dynasty famous medicine writer Meng Shen's "food therapy Materia Medica". Compared with drug therapy and surgery, the advantage of dietary therapy is that it has almost no toxic side effects on the body and reduces the invasiveness of substances such as hydrogels [9]. Research has shown that gut microbiota plays a role in the progression of SCI, but the studies about diet regulates intestinal flora metabolites to improve SCI are still limited and lack guiding significance. In addition, there is a lack of carriers for dietary regulation of intestinal microbiota and drug release.

Biomaterials of Zein protein are derived from corn and are versatile, low-cost, biocompatible and degradable. Current research indicates that Zein protein biomaterials are often prepared into nanoparticles for drug delivery [10]. Zein delivers excellent potential for biomedical applications. It was found that Zein can be loaded with IPA by using the nano-precipitation method. Evidence shows that Zein is very sensitive to digestive system degradation enzymes, resulting in an early release of IPA from Zein [11]. Pectin is a common food additive, which is a polygalacturonic acid polysaccharide found in citrus, lemon, grapefruit and other peels. However, pectin is

not digested by saliva, gastric juices and intestinal juices [12, 13]. A high-protein diet is recommended for the SCI treatment [14], zein and pectin are ideal for delivery carriers and diets.

Currently, spinal cord injury (SCI) induces disturbances in the gut microbiota, yet the exploration of the role of gut microbiota in the repair process following SCI remains limited. Previous studies have shown that resveratrol promotes the production of short-chain fatty acids, which are metabolites of the gut microbiota, and inhibits inflammatory responses after SCI [3]. Additionally, fecal microbiota transplantation from healthy individuals has been found to enhance motor function recovery after SCI by increasing the abundance of *Firmicutes*, *Blautia*, and *Anaerostipes* [7]. This suggests that the gut microbiota and its metabolites play a significant role in the repair process following SCI. Indole-propionic acid (IPA) is a metabolite of *Clostridium sporogenes*, a microbe found in the intestine. IPA has been shown to promote the regeneration of dorsal root ganglion neurons and to provide excellent neuroprotection [15, 16]. However, IPA appears to have a short half-life, which seems to limit its effectiveness [17]. In this study, we tried to load IPA (Pec-Zein-IPA NPs) in mice with SCI by using pectin and zein. IPA was slowly released to promote axon regeneration. Pec-Zein was involved in regulating intestinal microbial metabolites, reducing neuroinflammation and improving the microenvironment at the injured site. We assessed the levels of inflammation and oxidative stress after administration of Pec-Zein-IPA NPs in injured mice and evaluated axonal regeneration in the injured areas following SCI. We also examined the effects of intraintestinal Pec-Zein-IPA NPs on intestinal permeability, intestinal microorganisms and metabolites in mice following administration of these NPs. Collectively, the results of our study confirm that intestinal flora metabolites interfere with the microenvironment at the injured region, suggesting that Pec-Zein-IPA NPs can be beneficial for the treatment and management of SCI.

Materials and methods

Preparation of Pec-Zein and Pec-Zein-IPA NPs

Zein (240 mg) (aladdin, Z304904) was dissolved in 6 mL of 80% ethanol. The mixture was added to 20 mL of ultrapure water containing 1.25% sodium deoxycholate (SD) (aladdin, S104198) and stirred at 1000 g for 10 min. The amount of IPA (MCE, HY-W015229) added to Zein NPs was 0.1-1.0 mg/mL. Zein-IPA NPs solution was stirred at 800 g for 10 h to evaporate ethanol. Zein-IPA NPs were then placed in a dialysis bag (12000–14000 Da, Solarbio), PBS was added to 37°C and stirred for 1 h to remove free IPA and Zein-IPA NPs were obtained after freeze-drying. Pec-Zein-IPA NPs were prepared for animal experiments by mixing 60 mg pectin (aladdin, P112756) with 200 mL ultrapure water and stirring it for 30 min at 1000 g.

Characteristics of Zein-IPA NPs and Pec-Zein-IPA NPs

The Zein-IPA NPs and Pec-Zein-IPA NPs were dissolved in PBS and the particle size and Zeta potential were determined using the Zetasizer Nano ZS90. FEI Tecnai G2 F30 and SU8020 instruments were used to examine the Zein-IPA NPs and Pec-Zein-IPA NPs surface morphology.

The encapsulation efficiency and release of IPA in vitro and in vivo

Using FITC-labeled BSA (Solarbio, SF063) instead of IPA to observe drug release in vivo. Prepare Pec-Zein NPs loaded with FITC-labeled BSA using the above method. After freeze-drying the nanoparticles, reconstitute NPs for oral gavage administration to SCI mice. At corresponding time points, the mice were anesthetized with isoflurane, and images were captured using a small animal in vivo imaging system (IVIS Spectrum). Pepsin (Aladdin, P755347) and trypsin (Aladdin, E757753) were purchased from Aladdin to simulate the stomach and small intestine environment. As previously described [18], Zein-IPA NPs and Pec-Zein-IPA NPs were placed in a dialysis bag suspended in (100 mL PBS with 1% Tween80 and pepsin, pH 1.2) simulated gastric fluid (sgf) and stirred at 100 g to induce the gastric transport state at 37℃. To simulate the intestinal tract, the dialysis bags were suspended (100 mL PBS with 1% Tween 80 and trypsin, pH 6.8) and stirred at 100 g at 37°C. The dialysis bag was then placed in 100 mL PBS containing 1% Tween80, pH 7.4, harvested from a 20% microbiota filter and stirred at 37°C at 100 g. Next, the 2 mL PBS was collected after 0.5, 1, 2, 4, 8 and 24 h, respectively, and the new medium was added to PBS. NPs prepared with Zein-IPA were centrifuged at 4°C for 1 h using the BeckmanOtima100 instrument. Afterward, supernatant was collected and the absorbance of IPA was detected at 283 nm. The encapsulation of Zein-IPA NPs was finally calculated using the following formula:

$$\text{Encapsulation efficiency} = \left(1 - \frac{\text{the amount of free IPA in the supernatant}}{\text{the amount of total IPA}}\right)$$

Animals

Healthy two hundred female C57BL6/J mice were purchased from Gempharmatech Co.Ltd. and kept in standard conditions. The experimental protocols and procedures were approved by the Experimental Animal

Ethics Committee at Wenzhou Medical University, Zhejiang Province, (No. wydw2018-0043), and in accordance with the ARRIVE guidelines (Animals in Research: Reporting In Vivo Experiments) [19].

SCI mice and drug intervention

Female mice were fully anesthetized with isoflurane. Then, skin and muscles and the dorsal cord were exposed using an anesthesia machine. SCI model was established by using a vascular clamp for 1 min (30 g force, Oscar) after a T9-T10 segmental laminectomy [20]. The skin and muscles from back in the sham group were isolated without being injured. The mice were randomly allocated into groups of SCI, IPA, Pec-Zein NPs and Pec-Zein-IPA NPs. The mice in the IPA group received 40 mg/kg/day of IPA, while the mice in Pec-Zein-IPA group received nanoparticles (containing same amount of IPA compared to the IPA treatment group) daily. The mice of Pec-Zein group received the same nanoparticles without IPA and those in the SCI group received normal saline solution. The body function of all mice was restored by artificial bladder emptying twice daily following injury.

Motor function recovery

BMS scores were calculated according to the previously described method for 1, 3, 7, 14 dpi in mice following SCI [21]. The BMS score ranged from 0 (paralyzed) to 9 (normal) based on coordination, retro ankle range of motion, tail pose, trunk stability and sole pose. Neuroexam M-800 (medcomtech) was used to evaluate nerve function at the injured site 14 days after injury. Electrodes were placed on the gastrocnemius muscle of the hind limb to record the amplitude of the action potential.

HE and nissl staining

HE and Nissl staining kits (Solarbio) were used to stain the spinal cords of mice after the tissue was fixed and the 5 cm tissue sections were dewaxed and hydrated. The spinal cords were then stained as described in the kit instructions. The images were finally captured using a Nikon microscope.

Immunofluorescence staining

Spinal cord tissue sections were sufficiently dehydrated and blocked for endogenous catalase, repaired with sodium citrate under high pressure and incubated with primary antibody for Arg-1 (Proteintech, 66129-1-lg), GFAP (Santa Cruz Biotechnology, sc-33673), Neun (Abcam, ab104224), C-caspase 3 (Affinity, AF7022), iNOS (Abcam, ab178945), NF200 (Abcam, ab207176), TOM20 (Proteintech, 11802-1-AP), ZO-1 (Proteintech, 66452-1-lg) and Occludin (Proteintech, 27260-1-AP) at 4°C overnight. Next, tissue slide was adequately incubated with secondary antibody at room temperature for 1.5 h. DAPI-labeled nucleus and spinal cord images were obtained and analyzed by Nikon C2si and OLYMPUS VS200.

Western blot assay

The spinal cord protein was extracted using a protein extraction kit, isolated using Epizyme Biotech's 7.5-12.5% PAGE Gel Fast Preparation Kit (Epizyme Biotech) and transferred to PVDF membranes. Afterward, the samples were adequately blocked with QuickBlockTM Western (Beyotime) for 15 min and then incubated with primary antibodies such as Bcl-2 (Proteintech, 26593-1-AP), SOD2 (Proteintech, 24127-1-AP), NQO1 (Proteintech, 11451-1-AP), HO-1 (Proteintech, 10701-1-AP), Bax (Proteintech, 50599-2-lg), Nrf-2 (ZENBIOSCIENCE, 380773), p-AKT(ZENBIOSCIENCE, 381555), AKT (ZENBIOSCIENCE, R23412), p-p65 (ZENBIOSCIENCE, 310013), p65 (ZENBIOSCIENCE, 250060), p-mTOR (ZENBIOSCIENCE, 381557), mTOR (ZENBIOSCIENCE, 660108), NLRP3 (Abcam, 263899), Caspase1 (Affninty, AF4005), GSDMD (Affninty, AF4012), LC3 (HUABIO, ET1701-65), p62 (ZENBIOSCIENCE, 380612), SAMTOR (Proteintech, 21744-1-AP) and GAPDH (ZENBIOSCIENCE, 380626) overnight at 4°C. The secondary antibodies were then incubated for 2.5 h. The images of PVDF membranes were finally obtained using the chemiDoc XRS + software and quantified using Image Lab 5.2.

Quantitative RT-PCR (qRT-PCR)

Trizol (takera) reagent was used to extract total RNA from spinal cord tissue according to the supplier's instructions. cDNA was synthesized by PrimeScriptTM RT Master Mix (Takara) and qRT-PCR was performed using the TB green method. Finally, the mRNA expression was calculated and analyzed by $2-\Delta\Delta Ct$. Forward primer (5'-3'): IL-1β (TTTGAAGTTGACGGACCCCA A), CD86 (ACAGAGAGACTATCAACCTG), TNF-α (A CGGCATGGATCTCAAAGAC), GAPDH (GGCAAAT TCAACGGCACAGTCAAG), IL-6 (CTCCCAACAGAC CTGTCTATAC); Reverse primer (5'-3'): IL-1β (CACAG CTTCTCCACAGCCACA), CD86 (GAATTCCAATCA GCTGAGAAC), TNF-α (AGATAGCAAATCGGCTGA CG), GAPDH (TCGCTCCTGGAAGATGGTGATGG), IL-6 (CCATTGCACAACTCTTTTCTC).

Amplification, sequencing and analysis of 16S rRNA gene

Fecal (30 mg) were sequenced for 16S RNA analysis. The quality of DNA extraction was determined by 1.2% agarose gel electrophoresis after DNA extraction using Nanodrop. The Quant-iTPicoGreen dsDNA Assay Kit and Microplate Reader (BioTek, FLx800) were used to amplify the recovered products using a Fluorescence Assay Kit and PCR amplification. The samples were

mixed according to their sequencing quantities based on the fluorescence quantitative results. The sequencing libraries were prepared utilizing Illumina's TruSeq Nano DNA LT Library Prep Kit. Magnetic bead screening was used to remove joint self-contiguous segments and purification of the library system was performed after the addition of the joint. BECKMAN AMPure XP Beads were used to obtain the library enrichment products after amplifying the DNA fragments involved in splices by PCR. The library was finalized using 2% agarose gel electrophoresis to select and purify the fragments. The samples were sorted and categorized according to index and barcode information from the original sequence of quality preliminary screening. QIIME2 dada2 or Vsearch software analysis flows were followed for sequence denoising or OTU clustering. The sparse curve was evaluated using ASV/OUT distributions in different samples. ASV/OTU level distance matrix calculations, β and α diversity measurement were conducted using unsupervised sorting, clustering and statistical analyzing methods.

Extraction and analysis of fecal metabolites

A total of 25 female mice were were used for fecal metabolome analysis. The sample (50 mg) was placed in an EP tube with 2 medium steel balls. Then, 200 μL of pre-cooled 80% methanol aqueous solution was mixed and homogenized in a tissue breaker. Next, 800 μL was added, ultrasounded in an ice bath for 20 min and frozen at -20℃ for 1 h. The supernatant was obtained by centrifuging 16,000 g at 4°C for 20 min, then drying in high-speed vacuum enrichment centrifuges. Mass spectrometry analysis was performed with 100 mL of methanol-aqueous solution (1:1, v/v) redissolved and centrifuged for 15 min and the supernatant was collected for analysis. The sample volume was 4 μL, the column temperature was 40°C and the flow rate was 0.3 mL/min. For chromatographic gradient elution, the chromatographic mobile phase A is 0.1% formic acid solution and the mobile phase B is acetonitrile. In 2–6 min, B changes linearly from 0 to 48%. 6–10 min, B changed linearly from 48 to 100%; 10–12 min, B maintained at 100%; At 12–12.1 min, B changed linearly from 100 to 0% and at 12.1–15 min, B remained at 0%. The positive (+) and negative (-) modes of each sample were detected utilizing electrospray ionization (ESI). The samples were then separated by UPLC, analyzed by mass spectrometry using QE Plus mass spectrometer (Thermo Scientific) and ionized using an HESI source. Peak alignment, retention time correction and peak area extraction for raw data were performed using MSDIAL software. The total peak area of the positive and negative data for positive and negative ions was normalized, the peaks of the positive and negative ions were integrated and patterns were recognized using Python. The data were preprocessed by Unit variance scaling (UV) before being analyzed.

Fecal supernatant transplantation

For fecal transplantation, the feces of mice with SCI were collected and 50 mg feces were diluted with 1 mL sterile saline. The mixed sample was centrifuged at 100 g, 4℃, for 5 min, and the supernatant was filtered through 70 μm filter. SCI mice were given 100 μL fecal supernatant daily.

BV2 cells culture and drug treatment

The BV2 cells were purchased from Shanghai Zhongqiaoxinzhou Biotech (ZQ0397). BV2 cells were cultured in MEM medium with 10% fetal bovine serum, 1% penicillin-streptomycin solution and 5% CO_2 at 37°C. BV2 cells were treated with SAM or Met for 2 h after being divided into LPS + ATP, LPS + ATP + Met and LPS + ATP + SAM groups.

Intestinal permeability analysis

Briefly, the mice were fasted for 4 h at 14 dpi, and intragastric administration with 12 mg/20 g FITC-dextran (Sigma, FD4), then blood centrifugation was taken to obtain the supernatant after 4 h. The absorbance of the supernatant was analyzed at Em = 520 nm and Ex = 481 nm using a microplate reader.

Molecular docking

To evaluate the binding energy and interaction patterns of candidate SAM with SAMTOR, we employed AutodockVina 1.2.2, a computerized protein-ligand docking software. We from PubChem compound database (https://pubchem.ncbi.nlm.nih.gov/), SAM, Met and SAMTOR were downloaded from PDB (http://www.rcsb.org/). We first prepared the protein and ligand files, converted all the protein and molecular files to PDBQT format, removed all the water molecules, and added polar hydrogen atoms. The grid frame is centered to cover each protein domain and accommodate free molecular motion. Molecular docking studies by Autodock Vina 1.2.2 (http://autodock.scripps.edu/) is used to model visualization.

Statistical analysis

The analysis and modeling of multivariate data were performed using R (version 4.0.3) and R packages. The data were mean-centered using Pareto scaling. The models were developed using principal component analysis (PCA), orthogonal partial least-square discriminant analysis (PLS-DA), and partial least-square discriminant analysis (OPLS-DA). Permutation tests were performed to evaluate all models for overfitting. The OPLS-DA method was used to identify discriminating metabolites

Table 1 Zein NPs size with different concentration IPA

IPA (mg/mL)	Size (nm)	Polydispersity index (PDI)	Encapsulation efficiency (EE%)
0.6	548.2 ± 9	0.41 ± 0.04	77.14 ± 0.026
0.8	638.9 ± 52.55	0.5 ± 0.06	81.76 ± 0.56
1.0	651.7 ± 18.88	0.25 ± 0.01	85.2 ± 0.38

Table 2 The size of Zein, Zein-IPA and pec-Zein-IPA NPs

	Size (nm)	PDI
Zein NPs	388.8 ± 8.48	0.11 ± 0.03
Zein-IPA NPs	657.1 ± 18.8	0.25 ± 0.01
Pec-Zein-IPA NPs	671.2 ± 11.67	0.32 ± 0.02

based on the variable importance of projection (VIP). The discriminating metabolites were obtained using a statistically significant threshold of VIP values obtained from the OPLS-DA model and two-tailed Student's t test on the normalized raw data at univariate analysis level. Experimental data were analyzed using GraphPad Prism 8.0.2 software and were presented as mean ± SEM. ANOVA and Tukey's multiple comparison tests were used to compare two or more groups. VIP > 1, $p < 0.05$ was considered statistically significant.

Results

Characterization of Pec-Zein-IPA NPs and release of IPA

Our results suggest that intestinal flora and metabolites are disturbed after SCI in mice (Figure S1). In order to verify the therapeutic effect of food therapy on intestinal flora and SCI, pec-zein was synthesized to regulate intestinal flora and IPA release.The Pec-Zein-IPA NPs were freeze-dried after mixing zein with pectin and IPA. Tables 1 and 2 showed that Zein NPs containing 1 mg/mL IPA retained 85% IPA with an average particle size of 651.7 nm. It was found that Pec-Zein NPs with IPA had the average particle size of 671.2 nm and the potential of -22.47 (Fig. 1A-B). We found that Zein NPs did not significantly increase IPA encapsulation efficiency when the

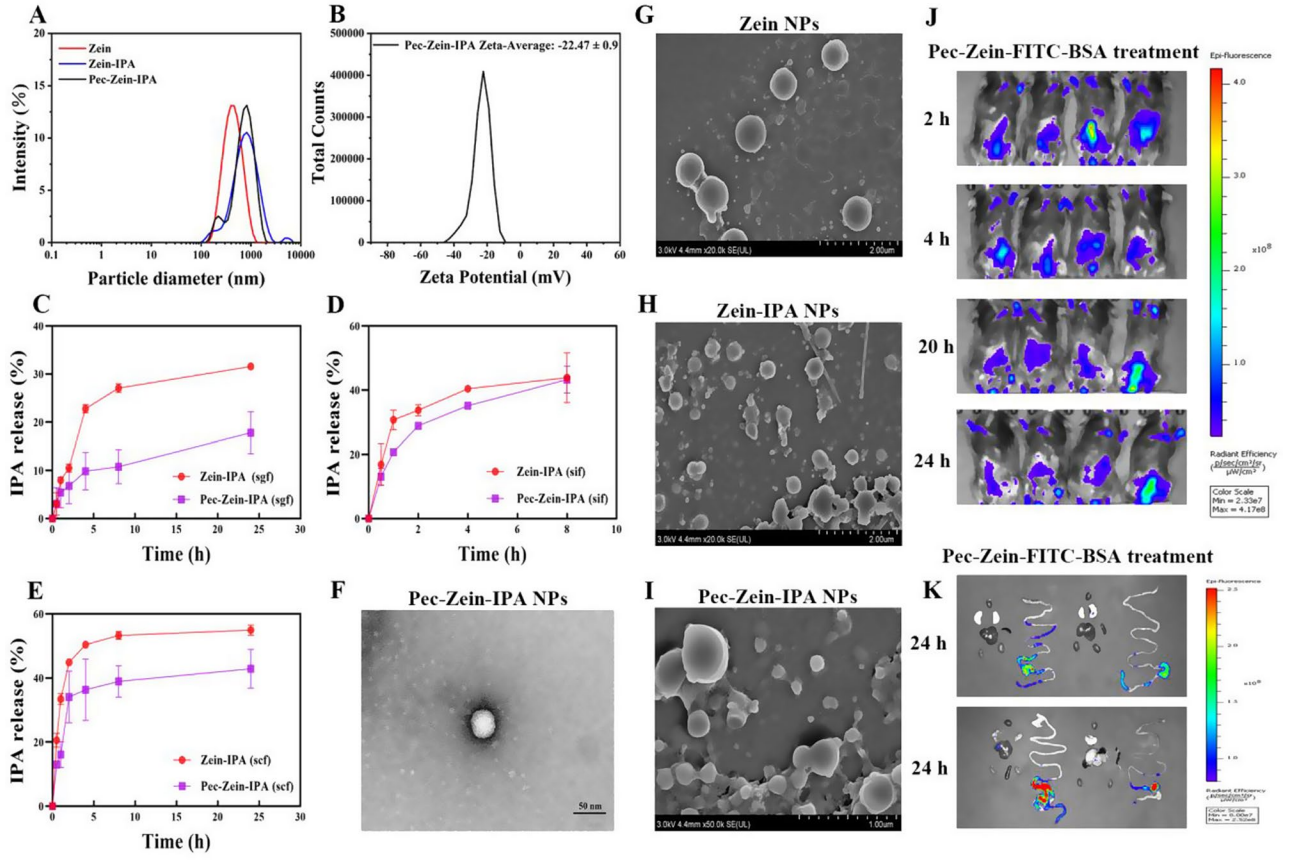

Fig. 1 Characterization and release of Zein-IPA and Pec-Zein-IPA NPs. (**A**) The NPs of Zein, Zein-IPA and Pec-Zein-IPA size. (**B**) The image of Pec-Zein-IPA NPs zeta potential. Zein NPs size with different concentration IPA. (**C**) Release of Pec-Zein-IPA and Zein-IPA NPs in the simulated gastric environment in vitro. (**D**) The release of Pec-Zein-IPA and Zein-IPA NPs in the simulated small intestine. (**E**) The release of Pec-Zein-IPA and Zein-IPA NPs in the simulated large intestine, $n = 3$ per group. (**F**) The TEM image of Pec-Zein-IPA NPs. (**G**-**I**) The SEM NPs of Zein, Zein-IPA and Pec-Zein-IPA, scale bar = 1 μm, 2 μm and 50 nm, respectively. (**J**) In vivo fluorescent images of SCI mice at different time points after Pec-Zein-FITC-BSA NPs treatment. (**K**) Imaging of Pec-Zein-FITC-BSA NPs in the heart, liver, spleen, lungs, kidneys, and intestines of mice 24 h after treatment for SCI

IPA concentration continued to increase, but the particle size increased. Therefore, we subsequently selected NPs containing IPA (1 mg/mL) to continue the experiment. Zein-IPA NPs and Pec-Zein-IPA NPs released IPA in the simulated stomach, small intestine and large intestine in vitro, demonstrating that the stomach could release a substantial amount of IPA (Fig. 1C-E). Taken together, the results indicated that Pec-Zein-IPA NPs are more suitable for administration. Additionally, we employed FITC-labeled BSA as a substitute for IPA in the sustained-release experiment for the gastrointestinal tract. In vivo imaging of small animals demonstrated that Pec-Zein-FITC-BSA NPs can achieve slow release in the intestine over a period of 24 h (Fig. 1J-K).

Pec-Zein-IPA NPs promoted motor function recovery in SCI mice

To evaluate histomorphologic altetions of Pec-Zein-IPA NPs intervention in SCI mice, we executed HE and Nissl staining. The HE staining at 7 and 14 days indicated that the SCI group lost more tissue than the sham group (Fig. 2B and C). In contrast, the Pec-Zein-IPA NPs treatment group exhibited a more complete tissue morphology. The results from the Nissl staining also indicated that neurons in the Pec-Zein-IPA group retained more neurons than in the SCI group (Fig. 2B). We further analyzed the promising effect of Pec-Zein-IPA NPs on motor function recovery in mice following SCI (Fig. 2E and F). The results showed that the BMS scores in the SCI model group were markedly reduced (Fig. 2G and H).

In contrast, the BMS scores in the Pec-Zein-IPA treatment group were augmented at 14 days compared to other injured groups. Our results showed that the amplitudes of the action potentials significantly correlated with the trend of BMS scores at 14 days post-injury (dpi) in the SCI group, but increased after treatment with Pec-Zein-IPA NPs in SCI group. Taken together, these results suggested that Pec-Zein-IPA NPs improved function recovery in injured mice.

Pec-Zein-IPA NPs inhibited the activation of OS and alleviated neuronal apoptosis in SCI mice

Reactive oxygen species (ROS) can induce OS and promote neuronal apoptosis following SCI. The level of ROS and apoptosis was determined in injured mice by

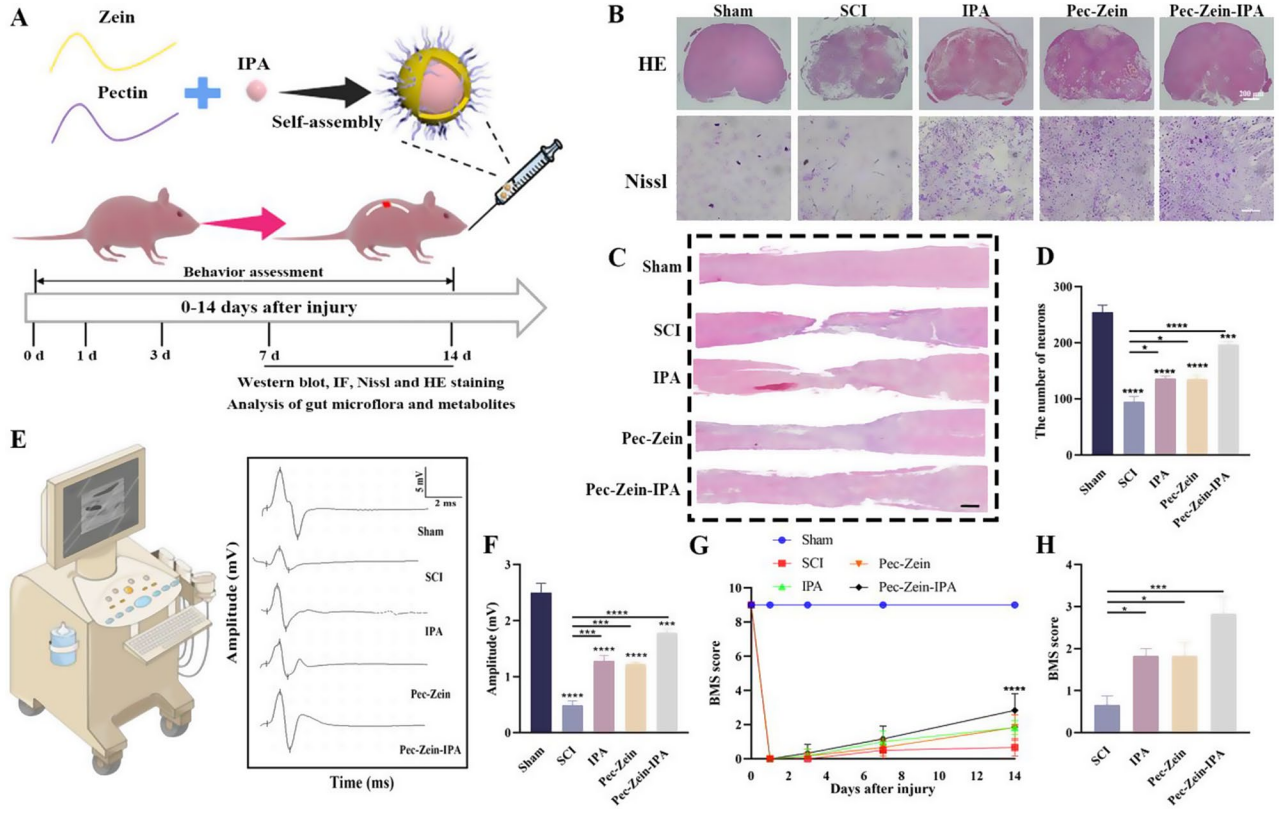

Fig. 2 (**A**) Experimental design and testing project diagram. (**B**) HE and Nissl results in each group at 7 dpi, scale bar = 200 μm, $n = 3$ per group. (**C**) The image of HE in each group at 14 dpi, scale bar = 500 μm, $n = 3$ per group. (**D**) Quantitative analysis of the number of neurons in each group, $n = 5$ per group. (**E**) The action potential amplitude in each group at 14 dpi, $n = 4$ per group. (**F**) Quantitative analysis from E, $n = 4$ per group. (**G**) BMS score in each group was 1, 3, 7, 14 dpi, and $n = 6$ per group. (**H**) Quantitative analysis of BMS score from G at 14 dpi in mice was $n = 6$ per group.*$p < 0.05$,***$p < 0.001$, ****$p < 0.0001$

DHE, western blotting and immunofluorescence staining, respectively. Immunofluorescence staining results indicated that Cleaved-caspase3 (C-caspase3) fluorescence intensity and DHE were significantly higher in the SCI group than in the sham group (Figure S2A, G). Our results also showed that the delivery Pec-Zein-IPA NPs significantly minimized the C-caspase3 and DHE fluorescence intensity. In addition, western blot assay revealed that Pec-Zein-IPA NPs treatment down-regulated the expression levels of pro-apoptotic protein Bax and up-regulated the expression levels of anti-apoptotic protein Bcl-2 and anti-oxidative stress-related proteins HO-1, NQO1 and SOD2 in mice following SCI (Figure S2B-K). Taken together, these results revealed that Pec-Zein-IPA could efficaciously inhibit the activation of OS and promote neuronal survival in mice following SCI.

Pec-Zein-IPA NPs alleviated neuroinflammation following SCI in mice

The release of several inflammatory factors following SCI further impairs the recovery of the injury [22–24]. Thus, we executed immunofluorescence staining to examine the expression of M1 and M2 microglia at the injured area in 7 and 14 days in mice following SCI. More importantly, figure S3A and B indicated that the fluorescence intensity of iNOS (M1-type microglia) was markedly enhanced between 7 and 14 days in SCI group. And we found that Pec-Zein-IPA NPs decreased the iNOS fluorescence intensity and enhanced the Arg-1 and CD206 (M2-type microglia) fluorescence intensity in mice following SCI. In addition, we further measured the mRNA expression levels of pro-inflammatory factor IL-6, TNF-α and IL-1β at 7 dpi in injured mice. The qRT-PCR analysis showed that the administration of IPA and Pec-Zein NPs down-regulated mRNA expression level of pro-inflammatory factor IL-6, TNF-α and IL-1β in mice following SCI. Furthermore, administration of Pec-Zein-IPA NPs also efficaciously suppressed the expression of pro-inflammatory factors in SCI mice (Figure S3E-G). Overall, above results confirmed that intervention of Pec-Zein-IPA NPs alleviated neuroinflammation in mice following SCI.

Pec-Zein-IPA NPs enhanced axon regeneration in mice following SCI

Previous study has shown that glial scars formation following SCI further hinders the regeneration of axons [25]. A recent study suggested that IPA significantly promoted axonal regeneration in the dorsal root ganglion neurons [15]. We utilized immunofluorescence staining to analyze whether IPA promoted axon regeneration in SCI region. Immunofluorescence result showed that the intensity of NF200 fluorescence was decreased in injured area at 14 days in SCI group. We found that IPA and Pec-Zein NPs could enhance the expression of NF200 in glial scar area. Intriguingly, the results also showed that Pec-Zein-IPA NPs further enhanced the expression of NF200 in damaged tissue regions in injued mice (Fig. 3A). Taken together, our findings indicated that Pec-Zein-IPA promoted axon regeneration in SCI mice.

Pec-Zein-IPA NPs treatment provided energy to promote axonal regeneration and activated the AKT/Nrf-2 signaling pathway

In our study, we demonstrated that IPA inhibits the activation of OS and protects neuronal survival. We investigated the underlying molecular mechanisms by which IPA suppresses the activation of OS. The results indicated that IPA treatment interfered with the AKT/Nrf-2 signaling pathway. Western blot assay showed that SCI down-regulated protein expression level of p-AKT and Nrf-2 compared with the sham group, whereas IPA intervention up-regulated these protein expression levels (Fig. 3B). Furthermore, we found that Pec-Zein and Pec-Zein-IPA NP administration significantly augmented protein expression level of p-AKT and Nrf-2 in injured mice. The administration of Pec-Zein-IPA NPs also downregulated the expression of endoplasmic reticulum stress-related protein GRP78 (Fig. 3B-I), which may be associated with the inhibition of OS. Study has demonstrated that oral energy supplies facilitate mitochondrial transfer and enhance axonal regeneration in injured tissue regions following SCI [26]. Based on the fact that Pectin and Zein are food-derived polysaccharides and proteins, we hypothesized that Pec-Zein-IPA NPs may also provide an additional source of energy to enhance SCI recovery. NF200, GFAP, and TOMM20 were used to label axons, glial scars and mitochondria, respectively. The results of immunofluorescence analysis confirmed that the administration of Pec-Zein and Pec-Zein-IPA NPs significantly enhanced the colocalization of TOMM20 and NF200 in the injured regions at 14 dpi (Fig. 3F). Taken together, above findings suggested that Pec-Zein-IPA NPs intervention provided energy and activated the AKT/Nrf-2 pathway in SCI mice.

Pec-Zein-IPA decreased intestinal permeability and attenuated intestinal inflammatory responses by inhibiting the activation of NF-κB signaling pathway

SCI further induces intestinal microbial imbalance, increases intestinal permeability and triggers intestinal inflammation [7]. Therefore, we employed the immunofluorescence technique to detect the intestinal barrier and FITC fluorescence in blood was examined by intragastric administration of FITC-labeled dextran at 14 days post-infection. The results revealed that intervention of Pec-Zein-IPA NPs reversed the reduction in intestinal compact connector protein ZO-1 and Occludin

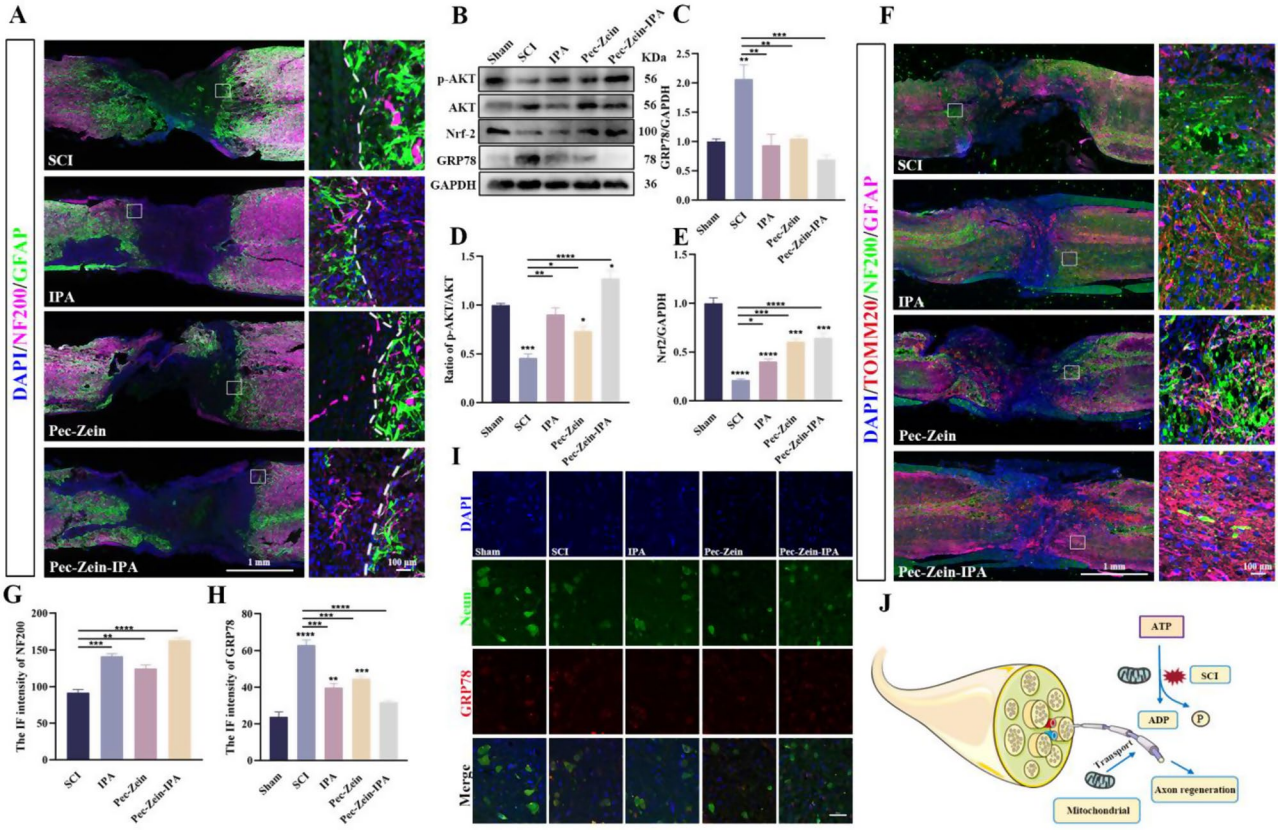

Fig. 3 Pec-Zein-IPA NPs promoted axonal regeneration and activated the AKT/Nrf-2 signaling pathway in SCI mice. (**A**) Immunofluorescence result of NF200 (Pink) and GFAP (green) in each group at 14 dpi, scale bar = 1 mm, 100 μm, respectively. (**B**) Western blot result of p-AKT, AKT, Nrf-2 and GRP78 in each group. (**C**-**E**) Quantitative analysis of membrane intensity of p-AKT, AKT, Nrf-2 and GRP78 in each group at 7 dpi, $n = 3$ per group. (**F**) Immunofluorescence image of NF200 (Green), GFAP (Pink) and TOMM20 (Red) in each group at 14 dpi, scale bar = 1 mm, 100 μm, respectively. (**I**) Immunofluorescence result of GRP78 (Red) and Neun (Green) in each group at 7 dpi, scale bar = 50 μm. (G-H) Quantitative analysis of immunofluorescence intensity NF200 and GRP78 from A and D at 7 dpi in mice, $n = 3$ per group. (**J**) Schematic diagram of the role of mitochondria in SCI. *$p < 0.05$, **$p < 0.01$, ***$p < 0.001$, ****$p < 0.0001$.

expression induced by SCI (Fig. 4A-C). We also detected high levels of FITC in the blood of SCI mice, whereas the levels of FITC in the Pec-Zein-IPA NPs treated group were significantly lower (Fig. 4D). We next analyzed mRNA expression level of pro-inflammatory factors IL-1β and TNF-α and activation of the NF-κB pathway in gut in SCI mice. Results of qRT-PCR and western blot analyses indicated that IPA and Pec-Zein NPs treatment down-regulated the ratio of p-p65/p65 proteins and the level of pro-inflammatory factors such as TNF-α and IL-1β in injured mice. Intriguingly, Pec-Zein-IPA NPs treatment group showed the similar results (Fig. 4E-H). Taken togther, our results indicated that intervention of Pec-Zein-IPA NPs decreased intestinal permeability and attenuated intestinal inflammatory responses following SCI in mice.

Pec-Zein-IPA NPs altered the composition of gut microbe after SCI

We performed 16S rRNA sequencing to determine whether Pec-Zein-IPA NPs have a regulatory effect on the intestinal microorganisms following SCI to further verify this hypothesis. Figure 5A demonstrates no significant difference between SCI and Pec-Zein-IPA NPs groups in α-diversity analysis (Fig. 5A). Intriguingly, Fig. 5D and E indicate that microbial communities differed following injury. It was observed that the abundances of *Fusobacteriota*, *Cyanobacteria*, *Actinbacteriota*, *Patescibacteria*, *Desulfobacterota*, *Bacteroidota*, *Firmicutes*, *Proteobacteria* and *Verrucomicobiota* were altered at the phylum level (Fig. 5B). We first selected the 20 microorganisms with considerable variation at the genus level including *Rikenella*, *Muribaculaceae*, *Colidextribacter* and *Escherichia_Shigella* (Fig. 5F). We found that SCI reduced the number of *Muribaculaceae* and increased *Candidatus_Saccharimonas*, *Bacterioides*, *Rikenella*, *Alistipes* and *Ligilactobacillus* compared

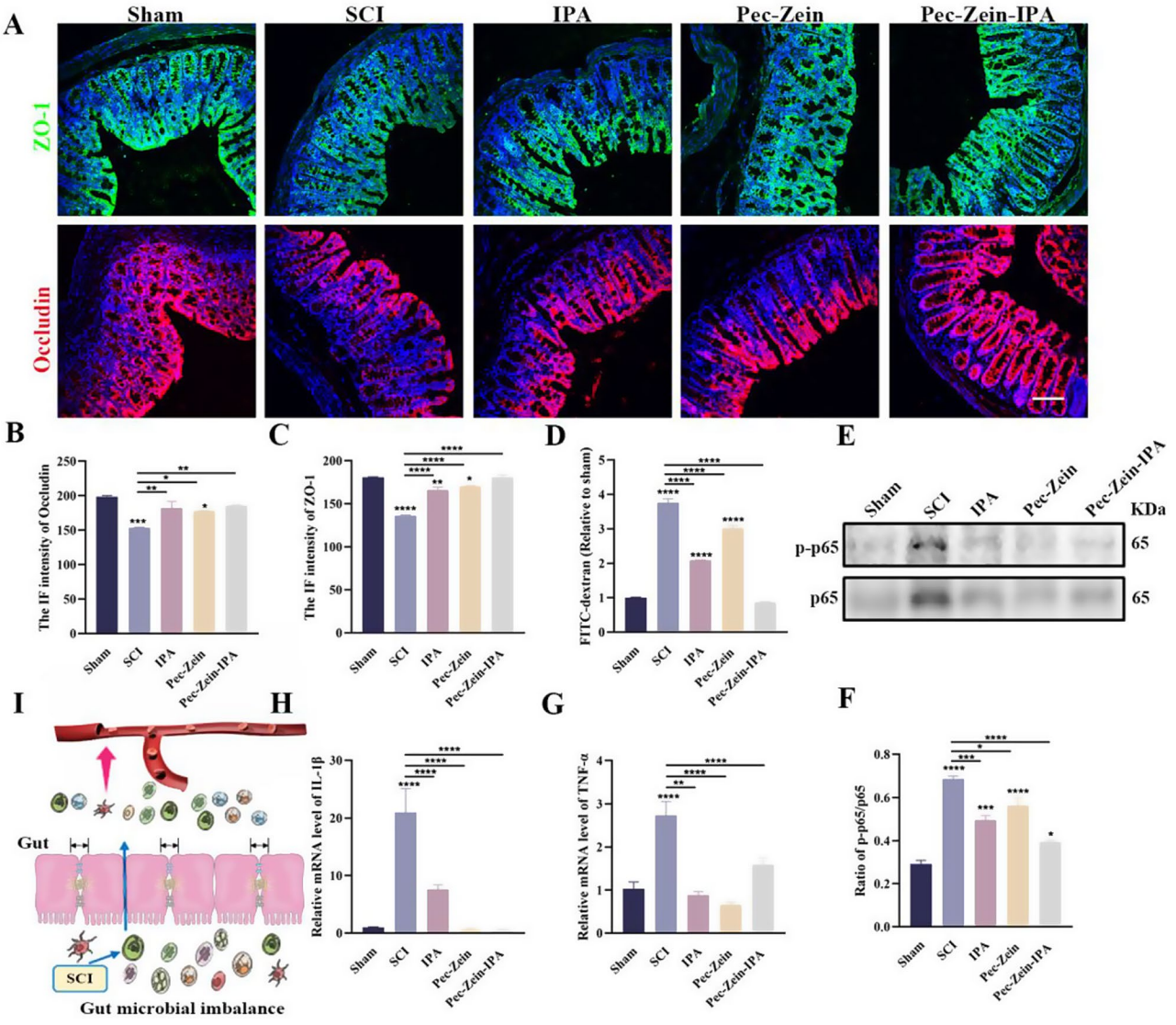

Fig. 4 Pec-Zein-IPA NPs decreased intestinal permeability and intestinal inflammatory responses by inhibiting NF-κB signaling pathways. (**A**) Immunofluorescence result of ZO-1 (Green), Occludin (Red) at 7 dpi in each group, scale bar = 50 μm. (**B**-**C**) Quantitative analysis of immunofluorescence intensity ZO-1 and Occludin, $n = 3$ per group. (**D**) Quantitative analysis of FITC-dextran in each group, $n = 5$ per group. (**E**) Western blot image of p-p65 and p65 at 7 dpi in each group. (**F**) Quantitative analysis ratio of p-p65/p65 from E, $n = 3$ per group. (**G**-**H**) Quantitative analysis expression of mRNA TNF-α, and IL-1β at 7 dpi in each group, $n = 3$ per group. (**I**) SCI leads to an imbalance of gut microbes. *$p < 0.05$, **$p < 0.01$, ***$p < 0.001$, ****$p < 0.0001$

to the Pec-Zein-IPA group. Our results showed that the Pec-Zein-IPA NPs group exhibited a lower abundance of *Firmicutes* and augmented the abundance of *Bacteroidata* and *Proteobacteria* at the phylum level compared to the SCI group. Furthermore, the results also showed that Pec-Zein-IPA treatment decreased the abundance of *Candidatus-Saccharimonas*, *Rikenella*, *Alistipes*, *Lachnospiraceae-NK4A136* and *Lachnospiraceae_UCG_001* at the genus level while dramatically increasing *Muribaculaceae*. The diagram illustrates the ratio of common and solitary species in each group based on the petals (Fig. 5I). In addition, our results also showed microorganisms with significant changes and statistical differences through LEFSe and heat maps (Fig. 5D, G). Overall, the above findings revealed that intervention of Pec-Zein-IPA NPs altered the composition of gut microbe in mice following SCI.

Pec-Zein-IPA NPs altered fecal metabolites after SCI

A growing body of evidence suggests that intestinal microbiota metabolites regulate the SCI prognosis and the intestinal microbiota is profoundly associated with the development of the nervous system [2, 3, 7, 27]. To investigate the effects of dietary therapy Pec-Zein on SCI, the SCI mice were treated with fecal flora supernatant transplantation from Pec-Zein and Pec-Zein-IPA groups.

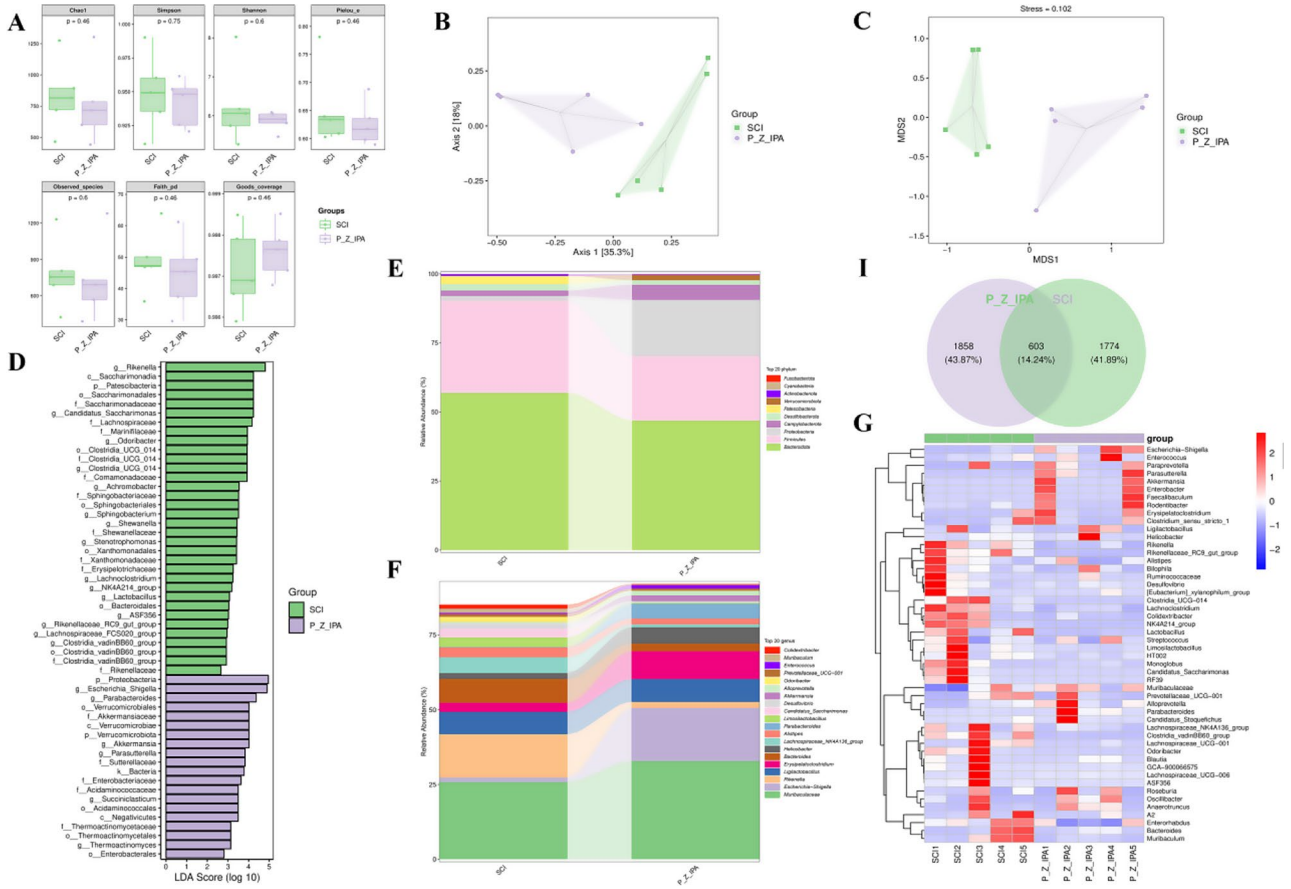

Fig. 5 Pec-Zein-IPA NPs altered gut microbe composition in mice following SCI. (**A**) The image of α-diversity with Chao1, Simpson, Shannon, Pielou_e, Observed_species, Faith-pd, and Goods_coverage, $n = 5$ per group. (**B**) Image of Bray-Curtis-based PcoA with the hull, $n = 5$ per group. (**C**) Image of Bray-Curtis based NMDS with hull, $n = 5$ per group. (**D**) Histogram of LDA effect values for marker species in each group. (**E**) Relative abundance at phylum levels for each group, $n = 5$ per group. (**F**) Relative abundance at genus levels for each group, $n = 5$ per group. (**G**) Generic level species composition heat map for species clustering. (**I**) Venn diagram for ASV/OTU

The results revealed that the mRNA expression levels of CD86 (M1-type microglia marker) and pro-inflammatory factors including IL-1β, IL-6 and TNF-α were markedly down-regulated in mouse feces from the Pec-Zein group and Pec-Zein-IPA group (Fig. 6A-E). Our results also demonstrated that gut microbial metabolites alleviated neuroinflammation following SCI in mice. We further analyzed the composition of metabolites in mouse feces. We identified 663 metabolites with significant variations. In addition, we identified 365 down-regulated and 298 up-regulated metabolites in the Pec-Zein-IPA group compared to the SCI group (Fig. 6F, G). KEGG pathway analysis revealed several amino acid metabolism-related metabolites including β-alanine, L-phenylalanine, L-Methionine, L-Glutamine, Tryptophan, Indole, Arginine, Tyrosine and L-isoleucine, which were substantially different (Fig. 7A). Based on microbiome and metabolite analysis, *Odoribacter*, *Candidatus_Saccharimonas*, *Clostridia_UCG-014*, *Shewanella*, *Escherichia_Shigella*, *Rikenella*, *Parabacteroides* and *Achromobacter* were positively and negatively correlated with these amino acids (Fig. 7A). We further identified elevated levels of creatine in the identified metabolites. We previously found that Pec-Zein promotes axonal regeneration following SCI and this energy supplier improves mitochondrial transport and axonal regeneration (Fig. 7A). Taken together, intervention of Pec-Zein-IPA NPs regulated fecal metabolites in mice following SCI.

Methionine (Met) increased inflammation levels in SCI mice

Previous study has shown that fecal metabolites L-Glutamine, L-Glutamate, L-Methionine, L-Valine, L-Tryptophan and L-Proline has significant changes in SCI mice at 21 dpi [6]. Accumulation of L-leucine, L-methionine, L-phenylalanine, L-isoleucine and L-valine was also observed in SCI mice [28]. Combined with our data analysis and screening, we found that L-Methionine had significant changes in feces and local injury sites after SCI in mice. Therefore, we speculated that L-Methionine might interfere with the molecular events of SCI. We further found that Met accumulation after SCI may exacerbate

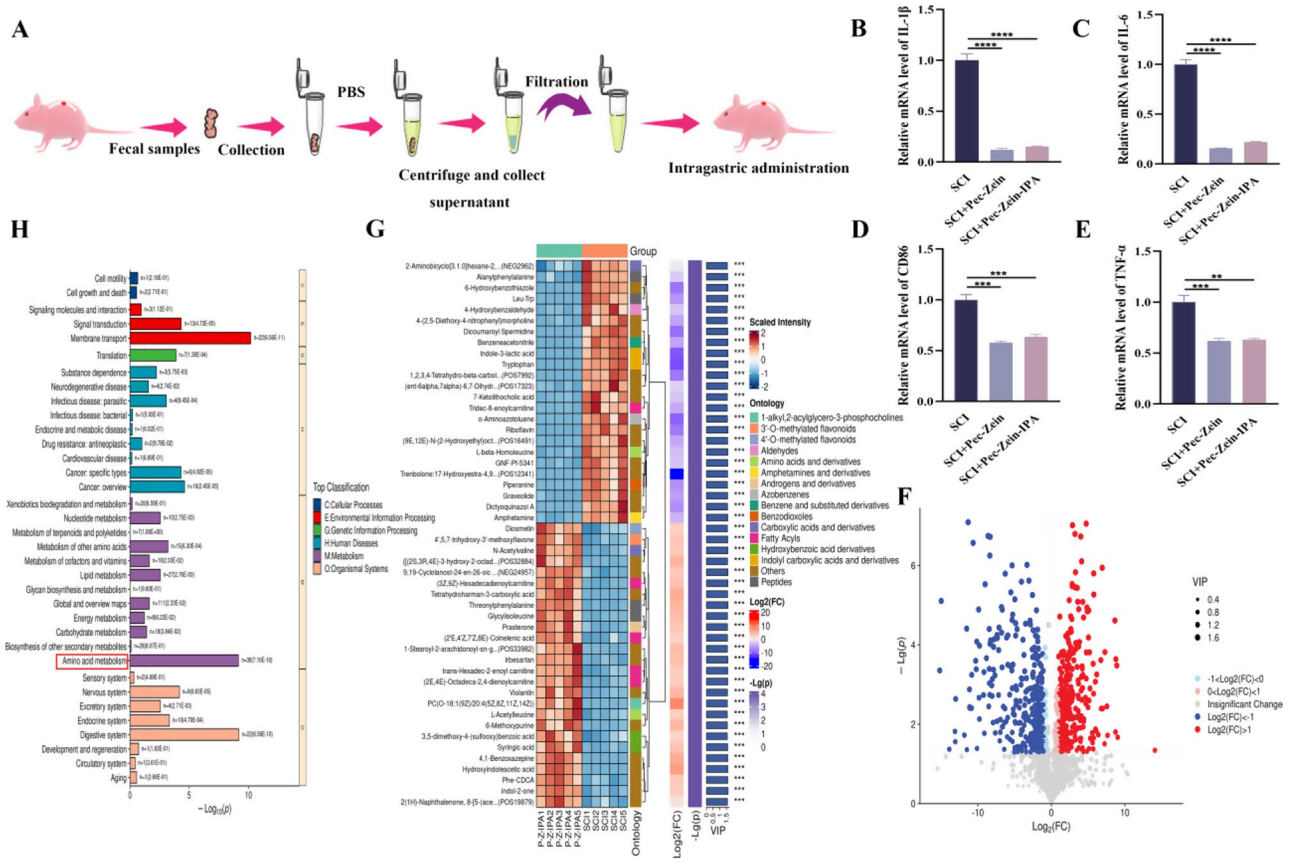

Fig. 6 Pec-Zein-IPA NPs altered microbiome compositionand fecal metabolites in SCI. (**A**) Schematic diagram of mouse feces treatment. (**B**-**E**) Quantitative analysis of mRNA CD86, TNF-α, IL-6, and IL-1β in SCI mice, $n = 3$ per group. (**F**) Volcanic map of Pec-Zein-IPA NPs vs. SCI group with red dots indicating up-regulated metabolites and blue dots indicating down-regulated metabolites, blue suggests decreased expression and red suggests increased expression. (**G**) Differential metabolite heat maps of Pec-Zein-IPA NPs and SCI groups, blue shows decreased expression and red shows increased expression. (**H**) Top classification KEGG pathway enrichment bar plot of Pec-Zein-IPA NPs vs. SCI group. $^{**}p < 0.01$, $^{***}p < 0.001$, $^{****}p < 0.0001$

neuroinflammation. We conducted qPCR analysis and the results showed that proinflammatory factors such as IL-1β, IL-6, and TNF-α were significantly upregulated, along with an increased expression level of CD86, a marker of M1-phenotype microglia (Fig. 7B-G). Based on KEGG and previous studies indicating that amino acids may be involved in autophagy pathways, we speculate that Met may affect neuroinflammation by regulating autophagy after SCI. To further analyze the mechanism of how Met exacerbates SCI neuroinflammation, we used western blotting to detect the expression levels of mTOR pathway and autophagy. Our results showed that Met significantly increased the activation of the mTOR pathway, upregulated the protein expression levels of the pyroptosis indicators caspase1 and GSDMD, but inhibited the level of autophagic flux after SCI in mice (Fig. 7H-I). We previously results found that Pec-Zein NPs treatment similarly alleviated neuroinflammation after SCI, and metabolome analysis showed that Pec-Zein NPs reduced L-methionine accumulation, suggesting that Pec-Zein NPs could improve inflammation in SCI by reducing L-methionine accumulation. We further analyzed the relevant intestinal flora, and our results showed that SCI resulted in a significant increase in the abundance of the flora *Clostridia_UCG-014*, *Clostridia_vadinBB60_group*, *Shewanella*, which are positively associated with L-methionine. Pec-Zein-IPA and Pec-Zein NPs treatment increased the abundance of associated bacteria and promoted the abundance of L-methionine negatively associated bacteria *Parasutterella* (Figure S4). Our results suggested that Pec-Zein-IPA may reduced neuroinflammation after SCI by regulating the abundance of these flora and altering L-methionine accumulation.

S-adenosylmethionine could directly induce microglial inflammation

To evaluate whether Met participated in autophagy and modulates inflammation, we conducted experiments in vitro using BV2 cells. We found that Met did not directly upregulate the levels of proinflammatory factors in LPS and ATP stimulated BV2 cells (Fig. 8A-B). We hypothesize that Met may not directly participate in autophagy

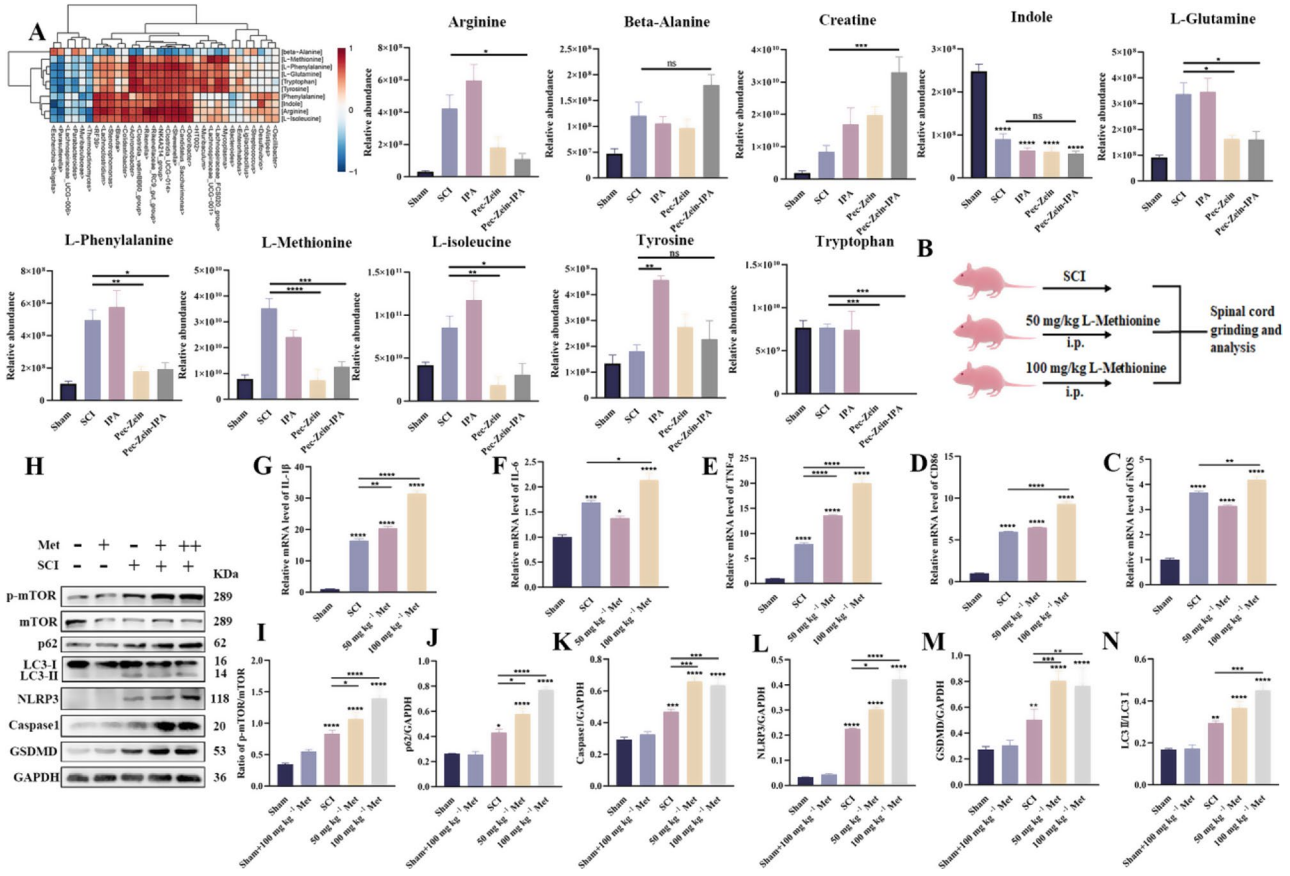

Fig. 7 Methionine increased inflammation levels in SCI mice in SCI. (**A**) Results of combined analysis of microbiome and metabolome, the blue suggests a negative correlation and red suggests a positive correlation. (**B**) Schematic diagram of mouse Met treatment. (**C**-**G**) Quantitative analysis of mRNA iNOS, CD86, TNF-α, IL-6, and IL-1β in mice, $n = 3$ per group. (**H**) Western blot image of p-mTOR, mTOR, p62, LC3, NLRP3, Caspase1, GSDMD and GAPDH at 3 and 5 dpi in each group. (**I**-**N**) Quantitative analysis p-mTOR, mTOR, p62, LC3, NLRP3, Caspase1 and GSDMD from H, $n = 3$ per group. $^{*}p < 0.05$, $^{**}p < 0.01$, $^{***}p < 0.001$, $^{****}p < 0.0001$

and inflammation regulation. Therefore, we investigated Met metabolite, S-adenosylmethionine (SAM), which is a direct metabolite produced by the enzymatic catalysis of methionine with ATP. Previous studies have shown that increased SAM concentrations can promote mTOR pathway activation [29]. Consequently, we further analyzed the role and mechanism of SAM in autophagy and inflammation. Our results demonstrate that SAM can directly increase the expression of proinflammatory factors IL-1β and IL-6 in LPS and ATP induced BV2 cells (Fig. 8C-D).

To elucidate the proinflammatory mechanism of SAM, we further analyzed how SAM regulated the mTOR pathway. Further molecular docking simulation results showed that SAM could be docked with SAMTOR, and the binding energies of SAM and MET were − 6.711 kcal/mol and − 4.436 kcal/mol, respectively, indicating that the binding of SAM and SAMTOR were stable (Fig. 8E, S5). Previous studies have shown that SAMTOR inhibits mTORC1 signaling by interacting with GATOR1 (GTPase-activating protein (GAP) for RagA/B), and that SAM can directly disrupt SAMTOR and GATOR1 interactions without the direct intervention of Met. This may explain why Met does not directly promote inflammation in BV2 cells while SAM does. Next, we used siRNA to silence SAMTOR in BV2 cells to evaluate the regulatory effect of SAM. Our results showed that SAM promoted mTOR pathway activation, significantly increased the pyroptosis level in BV2 cells, but inhibited autophagic flux (Fig. 8F-M). In the presence of siRNA, the expression levels of these proteins are even higher. In summary, our results suggest that increasing SAM concentration can alter the autophagy flow by regulating mTOR pathway, thereby promoting the release of inflammatory cytokines in BV2 cells. (Fig. 8N-P).

Discussion

Increasing evidence indicates that intestinal microbes play a role in central nervous system development and neurological diseases and loss of gastrointestinal control following SCI can exacerbate microenvironment homeostasis [3, 30]. In addition, SCI requires a lengthy recovery

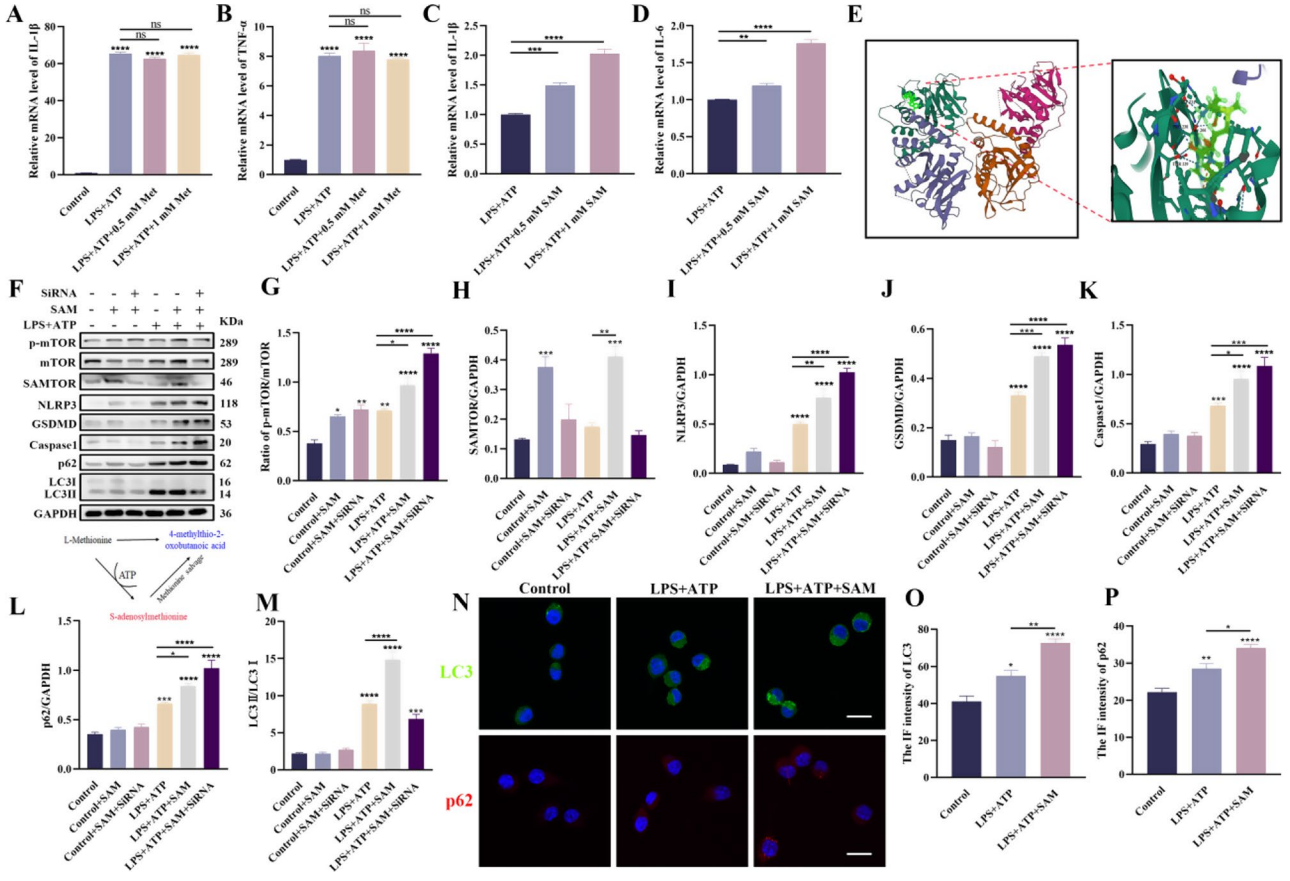

Fig. 8 SAM promoted neuroinflammation by regulating the mTOR pathway. (**A**-**D**) Quantitative analysis of mRNA proinflammatory factor RNA in LPS + ATP-stimulated BV2 cells. (**E**) Molecular docking diagram, SAM and SAMTOR interact and bond through visible hydrogen bonds and strong electrostatic interactions. (**F**) Western blot image of p-mTOR, mTOR, SAMTOR, p62, LC3, NLRP3, Caspase1, GSDMD and GAPDH in each group. (**G**-**M**) Quantitative analysis p-mTOR, mTOR, SAMTOR, p62, LC3, NLRP3, Caspase1 and GSDMD in LPS + ATP induced BV2 cells, $n = 3$ per group. (**N**) Immunofluorescence result of LC3 (Green), p62 (Red) in LPS + ATP induced BV2 cells, scale bar = 20 μm. $n = 3$ per group. (**O**-**P**) The IF intensity quantitative analysis of LC3 and p62. $^{*}p < 0.05$, $^{**}p < 0.01$, $^{***}p < 0.001$, $^{****}p < 0.0001$

period. Therefore, the regulation of gut microbes following SCI may be a safe and effective strategy for promoting endogenous nerve regeneration. However, how intestinal flora metabolite regulates the progression of SCI and which microbial flora metabolite plays a major role in it remains to be studied. Food therapy from ancient China and spread to the present day, can be used for disease prevention and disease treatment, and provide non-invasive methods of treatment, which has an important role in the development of safe and effective SCI treatment. In this study, we believe that the use of zein and pectin polysaccharide to provide energy and regulate metabolites of intestinal flora can improve the inflammatory environment at the injured site, and provide a good environment for IPA to promote axon regeneration.

The main treatment methods for SCI include surgical decompression therapy and medicine intervention. Currently, there is no specific and effective drug for the treatment of SCI. Clinically, high-dose intravenous infusion of the steroid medication methylprednisolone (MP) is used during the acute phase of SCI to alleviate symptoms [31]. However, MP only inhibits inflammation and does not exert neuroprotective effects, and its use is controversial [32–36]. Additionally, MP is associated with severe side effects including nausea, infection, and even patient death [31]. In mammals, there are often limitations to the

regeneration of mature neuronal axons. Current research rarely mentions any drugs that can promote axon regeneration or elucidate the underlying mechanisms. Indolepropionic acid (IPA), as an endogenous product in animals, is also present in human blood and has been reported to promote axon regeneration after sciatic nerve injury in mice [15, 37]. This suggests that IPA has potential therapeutic significance for SCI. In this study, our results showed that IPA treatment alleviated oxidative stress in neurons by activating the AKT/Nrf signaling pathway, promoted axonal regeneration, and improved functional recovery after SCI in mice, suggesting that intestinal microbiota metabolites played an important role in SCI. Therefore, we hypothesized that dietary regulation of intestinal flora metabolites could reduce inflammation at the SCI site and promote the recovery of motor function after SCI combined with IPA therapy. In this study, Pectin-Zein NPs were used as a drug carrier to deliver IPA through the intestine. Plant polysaccharides and fruit proteins such as pectin and zein have vast sources, are biocompatible and can be used as drug carriers in biomedical applications [38, 39]. Our results found that Pectin-Zein-IPA NPs increased neuronal survival, inhibited OS at the injured site, activated M2 glial cells and alleviated neuroinflammation following SCI in mice. Our study also demonstrated that Pectin-Zein-IPA NPs increased axonal regeneration following SCI compared with the IPA treatment group.

Based on the results of 16S rRNA sequencing and metabolomic analysis, although we confirmed that intestinal flora changes after SCI, intestinal flora metabolites are important factors involved in the pathological process in SCI. The analysis and verification of metabolites, we screened methionine and showed that the metabolite of methionine s-adenosylmethionine activates the mTOR pathway to inhibit autophagy and promote neuroinflammation by binding to SAMTOR (an S-adenosylmethionine sensor). Our results further suggested that Pec-Zein and Pec-Zein-IPA may reduced neuroinflammation after SCI by decreasing the abundance of *Clostridia_UCG-014*, *Clostridia_vadinBB60_group*, *Shewanella* (positively correlated with L-Methionine) and increasing the abundance of *Parasutterella* (negatively correlated with L-Methionine) and altering L-methionine accumulation. However, we have not yet verified which of these gut flora play a major role in L-methionine accumulation. We found that some amino acids accumulate abnormally. Specifically, the abnormal accumulation of phenylalanine and isoleucine in the periphery promotes immune cell infiltration and activates M1 microglia, leading to Alzheimer's disease-related neuroinflammation [40]. Glutamine metabolism regulates the activation of the NLRP3 inflammasome through mitophagy in microglia [41]. Arginine intervenes in intestinal inflammation by regulating macrophages [42]. These findings indicate that amino acid metabolism plays a crucial role in various diseases. However, the roles of these amino acids following SCI remain to be investigated.

Next, our results showed that methionine did not directly affect LPS + ATP-stimulated BV2 cells. We believed that this result may be caused by the short time of methionine pretreatment and the fact that methionine did not directly affect SAMTOR. To explore the factors most directly related to inflammation, therefore, we chose SAM and BV2 cells for validation instead of methionine. In this study, we found that Pectin-Zein-IPA NPs changed the gut microbiome immune axis, thereby altering the microenvironment at the injury site. Our results also found that although IPA can also be involved in altering intestinal microbiota metabolites, IPA has a smaller effect on amino acid metabolism. The above findings indicate that Pectin-Zein-IPA NPs may be advantageous in the management and treatment of SCI (Fig. 9). As an essential amino acid, L-methionine should be obtained by the body from food. Although intestinal flora may be involved in regulating L-methionine synthesis, we have not yet verified which intestinal flora play a major role in L-methionine synthesis after SCI. Our results suggest that reducing L-methionine uptake is beneficial for reducing neuroinflammation after SCI. Overall, our findings provide a strategy for drug treatment research in SCI. As a carrier, the natural ingredients in food arrive in the intestine in the form of nanoparticles loaded with drugs for safe and effective release, and can also be used as food to provide energy for long-term damage repair, which provides a reference for the transformation of scientific and technological achievements in the future.

In this study, we examined the composition of gut microbes and metabolites after the administration of Pec-Zein-IPA NPs to mice after SCI. Our results revealed that Pec-Zein-IPA NPs significantly altered amino acid metabolism of intestinal flora and that amino acids are involved in the life activities of immune cells. In addition, we could not explain how changes in other amino acids metabolism in intestinal microflora further affected immune cell function in the injured regions. Therefore, further investigations are highly required to determine whether these changes in other amino acids metabolism positively or negatively affect the immune system.

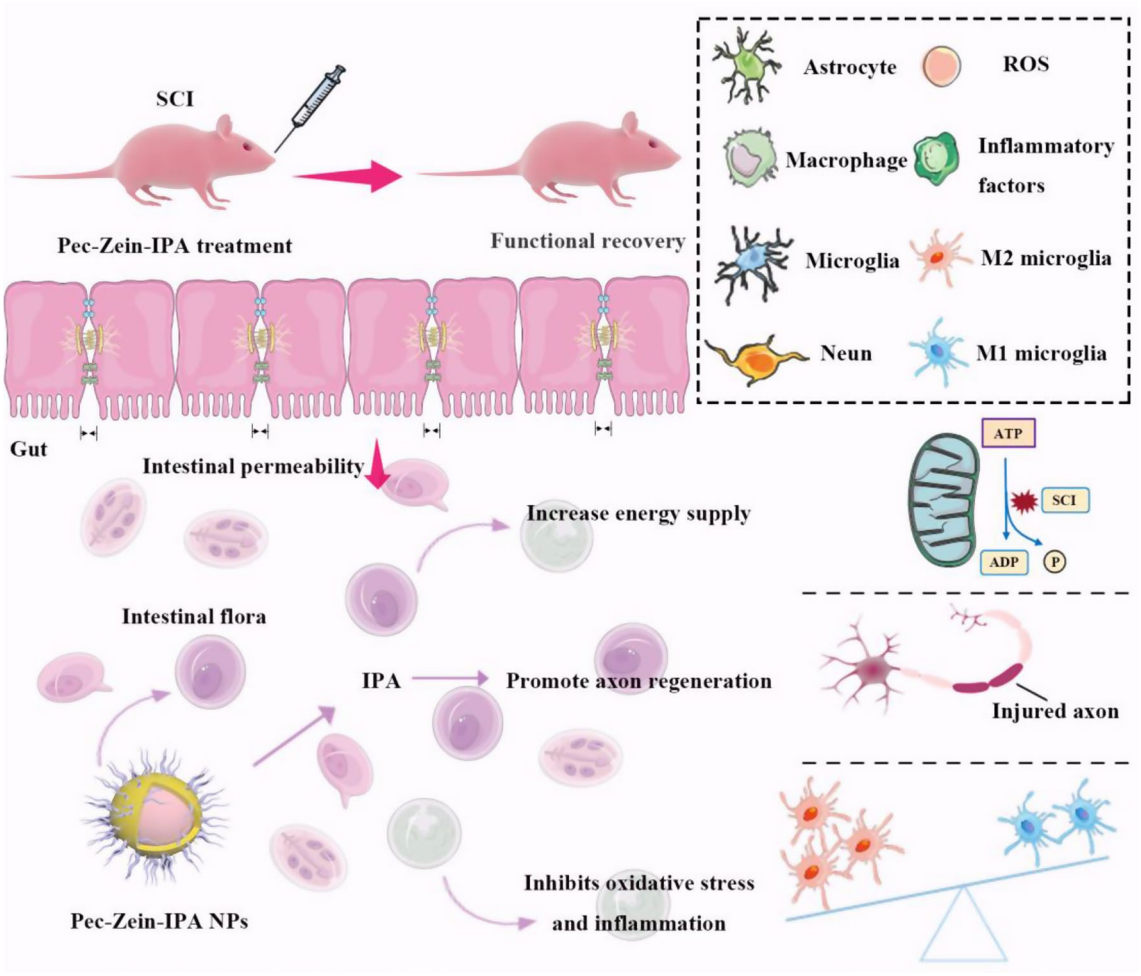

Fig. 9 A schematic diagram of Pec-Zein-IPA NPs promotes motor function recovery following SCI in mice

Conclusion

In our work, we successfully prepared Pec-Zein NPs to serve as carriers for IPA and further analyzed the characterization of the NPs. In vivo results suggested that Pec-Zein-IPA NPs could promote motor function recovery after SCI, and provide energy to promote axon regeneration, reduce neuroinflammation and oxidative stress, which may be related to intestinal flora and reducing L-methionine accumulation. Our results imply that Pec-Zein-IPA NPs are beneficial for the management and treatment of SCI. Reducing L-methionine intake can help reduce neuroinflammation after SCI.

Supplementary Information

The online version contains supplementary material available at https://doi.org/10.1186/s12951-025-03224-1.

Supplementary Material 1

Acknowledgements
We thank Shanghai Bioprofile Technology Co., Ltd. for technical support in mass spectroscopy. Thanks to Figdraw for the Graphical abstract drawing help. The author extends their gratitude to the Home for Researchers (http://www.home-for-researchers.com) for their assistance with the molecular docking.

Author contributions
Authors' contributions: Conceptualization: Xianghang Chen, Jian XiaoMethodology: Xianghang Chen, Beini Wang, Kaiyi Du, Shengfu WangInvestigation: Xianghang Chen, Siwang Hu, Qianqian Hu, Xinyuan Chen, Anyu Du, Jiaqin Shao, Yang Lu Visualization: Xianghang Chen, Kailiang Zhou, Yueqi Wu, Jiaqin ShaoWriting—original draft: Xianghang Chen, Shuangshuang Wang, Chang JiangWriting—review & editing: Abdullah Al Mamun, Jian Xiao.

Funding
This work was supported by the National Natural Science Foundation of China (82172428), the Natural Science Foundation of Zhejiang Provincial (LZ23H060001) and Zhejiang Provincial Program for Medicine and Health (2022KY446, 2023KY1345, 2023KY1347).

Data availability
All data are available in the main text or the supplementary materials. Please contact the corresponding author for data requests.

Data availability
No datasets were generated or analysed during the current study.

Declarations

Ethics approval and consent to participate

The experimental protocols and procedures were approved by the Experimental Animal Ethics Committee at Wenzhou Medical University, Zhejiang Province, (No. wydw2018-0043), and in accordance with the ARRIVE guidelines (Animals in Research: Reporting In Vivo Experiments) [19].

Consent for publication

Not applicable.

Competing interests

The authors declare no competing interests.

Author details

[1]Department of Arthroplasty, The First People's Hospital of Wenling, The Affiliated Wenling Hospital of Wenzhou Medical University, Taizhou, Zhejiang 317500, China
[2]Oujiang Laboratory (Zhejiang Lab for Regenerative Medicine, Vision and Brain Health), School of Pharmaceutical Sciences, Wenzhou Medical University, Wenzhou, Zhejiang 325035, China
[3]College of Nursing, Wenzhou Medical University, Wenzhou, Zhejiang 325000, China
[4]Department of Orthopaedics, The Second Affiliated Hospital, Yuying Children's Hospital of Wenzhou Medical University, Wenzhou 325027, China

Received: 4 December 2024 / Accepted: 11 February 2025
Published online: 28 February 2025

References

1. Feng X, Chen X, Zaeem M, et al. Sesamol attenuates neuroinflammation by regulating the AMPK/SIRT1/NF-kappaB signaling pathway after spinal cord Injury in mice. Oxid Med Cell Longev. 2022;2022:8010670.
2. Jing Y, Yang D, Bai F, et al. Spinal cord injury-induced gut dysbiosis influences neurological recovery partly through short-chain fatty acids. NPJ Biofilms Microbiomes. 2023;9(1):99.
3. He N, Shen G, Jin X, et al. Resveratrol suppresses microglial activation and promotes functional recovery of traumatic spinal cord via improving intestinal microbiota. Pharmacol Res. 2022;183:106377.
4. Kong G, Zhang W, Zhang S, et al. The gut microbiota and metabolite profiles are altered in patients with spinal cord injury. Mol Brain. 2023;16(1):26.
5. Li J, Van Der Pol W, Eraslan M, et al. Comparison of the gut microbiome composition among individuals with acute or long-standing spinal cord injury vs. able-bodied controls. J Spinal Cord Med. 2022;45(1):91–9.
6. Rong ZJ, Cai HH, Wang H, et al. Ursolic acid ameliorates spinal cord Injury in mice by regulating gut microbiota and metabolic changes. Front Cell Neurosci. 2022;16:872935.
7. Jing Y, Yu Y, Bai F, et al. Effect of fecal microbiota transplantation on neurological restoration in a spinal cord injury mouse model: involvement of brain-gut axis. Microbiome. 2021;9(1):59.
8. Kigerl KA, Hall JC, Wang L, et al. Gut dysbiosis impairs recovery after spinal cord injury. J Exp Med. 2016;213(12):2603–20.
9. Moravejolahkami AR, Chitsaz A, Hassanzadeh A, et al. Effects of Anti-inflammatory-antioxidant-rich diet and co-supplemented synbiotics intervention in patients with progressive forms of multiple sclerosis: a single-center, single-blind randomized clinical trial. Nutr Neurosci. 2023;26(11):1078–89.
10. Chen X, Wang B, Mao Y et al. Zein nanoparticles loaded with chloroquine improve functional recovery and attenuate neuroinflammation after spinal cord injury. Chem Eng J. 2022;450.
11. Li M, Yu M. Development of a nanoparticle delivery system based on zein/polysaccharide complexes. J Food Sci. 2020;85(12):4108–17.
12. Houron C, Ciocan D, Trainel N et al. Gut microbiota reshaped by Pectin Treatment improves liver steatosis in obese mice. Nutrients. 2021;13(11).
13. Ren Y, Mao S, Zeng Y et al. Pectin from Citrus Unshiu Marc. Alleviates glucose and lipid metabolism by regulating the gut microbiota and metabolites. Foods. 2023;12(22).
14. Raue KD, David BT, Fessler RG. Spinal cord-gut-Immune Axis and its implications regarding Therapeutic Development for spinal Cord Injury. J Neurotrauma. 2023;40(9–10):793–806.
15. Serger E, Luengo-Gutierrez L, Chadwick JS, et al. The gut metabolite indole-3 propionate promotes nerve regeneration and repair. Nature. 2022;607(7919):585–92.
16. Pappolla MA, Perry G, Fang X, et al. Indoles as essential mediators in the gut-brain axis. Their role in Alzheimer's disease. Neurobiol Dis. 2021;156:105403.
17. Wikoff WR, Anfora AT, Liu J, et al. Metabolomics analysis reveals large effects of gut microflora on mammalian blood metabolites. Proc Natl Acad Sci U S A. 2009;106(10):3698–703.
18. Wu A, Chen C, Lu J, et al. Preparation of oral core-Shell Zein Nanoparticles to improve the bioavailability of Glycyrrhizic Acid for the treatment of Ulcerative colitis. Biomacromolecules. 2022;23(1):210–25.
19. Kilkenny C, Browne WJ, Cuthill IC, et al. Improving bioscience research reporting: the ARRIVE guidelines for reporting animal research. PLoS Biol. 2010;8(6):e1000412.
20. Jiang W, Li M, He F, et al. Inhibition of NLRP3 inflammasome attenuates spinal cord injury-induced lung injury in mice. J Cell Physiol. 2019;234(5):6012–22.
21. Basso DM, Fisher LC, Anderson AJ, et al. Basso Mouse Scale for locomotion detects differences in recovery after spinal cord injury in five common mouse strains. J Neurotrauma. 2006;23(5):635–59.
22. Francos-Quijorna I, Sanchez-Petidier M, Burnside ER, et al. Chondroitin sulfate proteoglycans prevent immune cell phenotypic conversion and inflammation resolution via TLR4 in rodent models of spinal cord injury. Nat Commun. 2022;13(1):2933.
23. Ji ZS, Gao GB, Ma YM, et al. Highly bioactive iridium metal-complex alleviates spinal cord injury via ROS scavenging and inflammation reduction. Biomaterials. 2022;284:121481.
24. Shen K, Sun G, Chan L, et al. Anti-inflammatory nanotherapeutics by targeting Matrix metalloproteinases for Immunotherapy of spinal Cord Injury. Small. 2021;17(41):e2102102.
25. Sun Y, Liu Q, Qin Y, et al. Exosomes derived from CD271(+)CD56(+) bone marrow mesenchymal stem cell subpopoulation identified by single-cell RNA sequencing promote axon regeneration after spinal cord injury. Theranostics. 2024;14(2):510–27.
26. Han Q, Xie Y, Ordaz JD, et al. Restoring Cellular Energetics promotes axonal regeneration and functional recovery after spinal Cord Injury. Cell Metab. 2020;31(3):623–41. e8.
27. Wang J, Zhao X, Zhou R, et al. Gut microbiota and transcriptome dynamics in every-other-day fasting are associated with neuroprotection in rats with spinal cord injury. Front Microbiol. 2023;14:1206909.
28. Kang JN, Sun ZF, Li XY, et al. Alterations in gut microbiota are related to metabolite profiles in spinal cord injury. Neural Regen Res. 2023;18(5):1076–83.
29. Gu X, Orozco JM, Saxton RA, et al. SAMTOR is an S-adenosylmethionine sensor for the mTORC1 pathway. Science. 2017;358(6364):813–8.
30. Gur Arie A, Toren T, Hadar R, et al. Lack of gut microbiome recovery with spinal cord injury rehabilitation. Gut Microbes. 2024;16(1):2309682.
31. Baroudi M, Rezk A, Daher M, et al. Management of traumatic spinal cord injury: a current concepts review of contemporary and future treatment. Injury. 2024;55(6):111472.
32. Guan B, Fan Y, Zheng R, et al. A critical appraisal of clinical practice guidelines on pharmacological treatments for spinal cord injury. Spine J. 2023;23(3):392–402.
33. Lee BJ, Jeong JH, Review. Steroid use in patients with Acute spinal cord Injury and Guideline update. Korean J Neurotrauma. 2022;18(1):22–30.
34. Martirosyan NL. Pharmacologic and cell-based therapies for Acute spinal cord Injury. Neurosurg Clin N Am. 2021;32(3):389–95.
35. Takami T, Shimokawa N, Parthiban J, et al. Pharmacologic and regenerative cell therapy for spinal cord Injury: WFNS Spine Committee recommendations. Neurospine. 2020;17(4):785–96.
36. Thomas AX, Riviello JJ Jr., Davila-Williams D, et al. Pharmacologic and Acute Management of spinal cord Injury in adults and children. Curr Treat Options Neurol. 2022;24(7):285–304.
37. Yao L, Devotta H, Li J, et al. Dysrupted microbial tryptophan metabolism associates with SARS-CoV-2 acute inflammatory responses and long COVID. Gut Microbes. 2024;16(1):2429754.
38. Yang Z, Zhang Y, Jin G, et al. Insights into the impact of modification methods on the structural characteristics and health functions of pectin: a comprehensive review. Int J Biol Macromol. 2024;261(Pt 2):129851.
39. Wang D, Wang J, Wu Y, et al. Amelioration of Acute Alcoholic Liver Injury via attenuating oxidative damage and modulating inflammation by means of Ursodeoxycholic Acid-Zein nanoparticles. J Agric Food Chem. 2023;71(45):17080–96.

40. Wang X, Sun G, Feng T, et al. Sodium oligomannate therapeutically remodels gut microbiota and suppresses gut bacterial amino acids-shaped neuroinflammation to inhibit Alzheimer's disease progression. Cell Res. 2019;29(10):787–803.
41. Zhang Z, Li M, Li X, et al. Glutamine metabolism modulates microglial NLRP3 inflammasome activity through mitophagy in Alzheimer's disease. J Neuroinflammation. 2024;21(1):261.
42. Xu X, Ocansey DKW, Pei B, et al. Resveratrol alleviates DSS-induced IBD in mice by regulating the intestinal microbiota-macrophage-arginine metabolism axis. Eur J Med Res. 2023;28(1):319.

Publisher's note